

Synthesis and Characterization of Cyclic Cationic Polymer and its Anti-corrosion Property for Low Carbon Steel in 15% HCl Solution

Shamsuddeen A. Haladu¹, Saviour A. Umoren^{2,*}, Shaikh A. Ali³, Moses M. Solomon⁴

¹ Department Basic Sciences, College of Engineering, University of Dammam, Saudi Arabia

² Centre of Research Excellence in Corrosion, Research Institute, King Fahd University of Petroleum and Minerals, Dhahran 31261, Saudi Arabia

³ Department of Chemistry, King Fahd University of Petroleum & Minerals, Dhahran 31261, Saudi Arabia

⁴ Corrosion Research Laboratory, Department of Mechanical Engineering, Faculty of Engineering, Duzce University, 81620 Duzce, Turkey

*Email: umoren@kfupm.edu.sa

Received: 28 April 2017 / Accepted: 6 August 2017 / Published: 12 September 2017

A new cyclic cationic polymer (CCP) bearing bis-3-phosphorylpropyl pendants was synthesized using chain-growth polymerization technique with ammonium persulphate (APS) as initiator. The synthesized polymer was characterized using FTIR, ¹H NMR and ¹³C NMR techniques. The corrosion inhibition performance evaluation of the newly synthesized polymer for low carbon steel in 15% HCl was carried out using weight loss measurements at 25 – 60 °C, electrochemical impedance spectroscopy (EIS), potentiodynamic polarization (PDP) and linear polarization resistance (LPR) techniques. The effect of addition of small amounts (5 mM) of ZnCl₂ and KI on the corrosion inhibition performance of CCP was also assessed. Results obtained indicate that CCP acts as an inhibitor for low carbon steel corrosion in the aggressive acid environment. Inhibition efficiency increased slightly with increasing CCP concentration. Also, inhibition efficiency was found to decrease with increase in temperature. Addition of ZnCl₂ and KI to CCP has profound effect on the corrosion inhibition performance, which was more pronounced with KI compared to ZnCl₂. Corrosion protection efficiency followed the trend CCP + KI > CCP + ZnCl₂ > CCP. The enhanced corrosion inhibition of CCP on addition of ZnCl₂ and KI is due to synergistic effect as confirmed from the calculated synergistic parameter which was found to be greater than unity. Inhibition of low carbon steel corrosion in 15% HCl occurs by virtue of physical adsorption of CCP onto the steel surface which can be approximated by Langmuir adsorption isotherm model. The SEM/EDS images confirm the adsorption of CCP to form protective film on the low carbon steel surface.

Keywords: Polymer; Hydrochloric acid; steel; Acid corrosion; Corrosion inhibition; Synergism

1. INTRODUCTION

Corrosion of mild steel remains a phenomenon of great concern owing to its widespread use as a construction material in various industries and the fact that it corrodes easily in acidic media. In the petroleum industry, acidizing is an indispensable step in the drilling operation. In the process, strong acid solutions are forced through carbon steel tubing into the well to open up near bore channels in the formation and to increase the flow of oil. Several acid-based stimulation fluids are used in the acidization process. Among various mineral acids, HCl (15% to 28%) is prevalently used in the stimulation of carbonate based petroleum oil reservoirs [1-3] since it cheap and forms water soluble metal chloride [3, 4].

The addition of corrosion inhibitors to the aggressive acid solutions is a must in order to protect oil and gas well equipment from corroding during the acidization process. The commonly used corrosion inhibitors in petroleum oil/gas field applications are organic compounds that contain heteroatoms like nitrogen, sulfur, oxygen, phosphorus and multiple bonds [5, 6]. The inhibition efficiency increases in the order $O < N < S < P$ [6]. The inhibition mechanism of the compounds is ascribed to their adsorption on the metal surface, thus, forming a protective film that hampers anodic/cathodic reactions on the metal thereby mitigating the corrosion process [7]

There exists a diverse list of organic compounds studied as corrosion inhibitors for mild steel in 15% HCl solution. Among them are, spiropyrimidinethiones [2], alcohol-based inhibitors [4], benzimidazole derivatives [5], pyranopyrazole derivatives [8], trans-cinnamaldehyde [9], imidazole derivatives [10], cationic gemini surfactants [11], pyridine derivatives [12], pyrazolone derivatives [13], S-N Schiff bases [14], benzyl quinolinium chloride derivative [15] and amino acid derivatives [16].

Recently, exploration of a variety of polymers as corrosion inhibitors for mild steel has become the focus of research [17-23] due to the presence of multiple adsorption sites in the polymer, handiness, cost effectiveness, safe in handling and environmental friendliness [24]. However, quite few studies have been reported on the application of polymers as corrosion inhibitors for steel in strong acid such as 15% HCl solution used in matrix stimulation and acid fracturing. To our knowledge, the literature has documented only two relevant polymer based materials namely xanthan gum and its graft co-polymer [25] and polypropylene glycol [26] as corrosion inhibitors for mild steel in 15% HCl.

In view of such advantages of polymers and our quest for more potent polymeric corrosion inhibitors in hostile environments, the present work reports the synthesis of a cyclic cationic polymer bearing bis-3-phosphorylpropyl pendants (Scheme 1) and its corrosion inhibition efficiency in 15% HCl solution for low carbon steel. The effect of addition of zinc and iodide ions on the efficiency of the polymer was also investigated. Both weight loss and electrochemical methods were employed followed by surface morphological analysis. Our previous work has reported the cyclopolymer as an efficient antiscalant [27]. The current polymer, being an aminophosphonate was envisaged to arrest corrosion due to the presence of phosphonate group, which is known to be an effective chelating agent, having hydrolytic stability; enabling it to find multitude of applications such as corrosion inhibitors for various metals, scale inhibitors, pulp production and bleaching of paper and textiles[28-30]. Some

phosphonates find applications in medicine: As drug contents for treatment of diseases such as HIV and hepatitis B [31], to treat bone-related disorders [32] and dental applications [33].

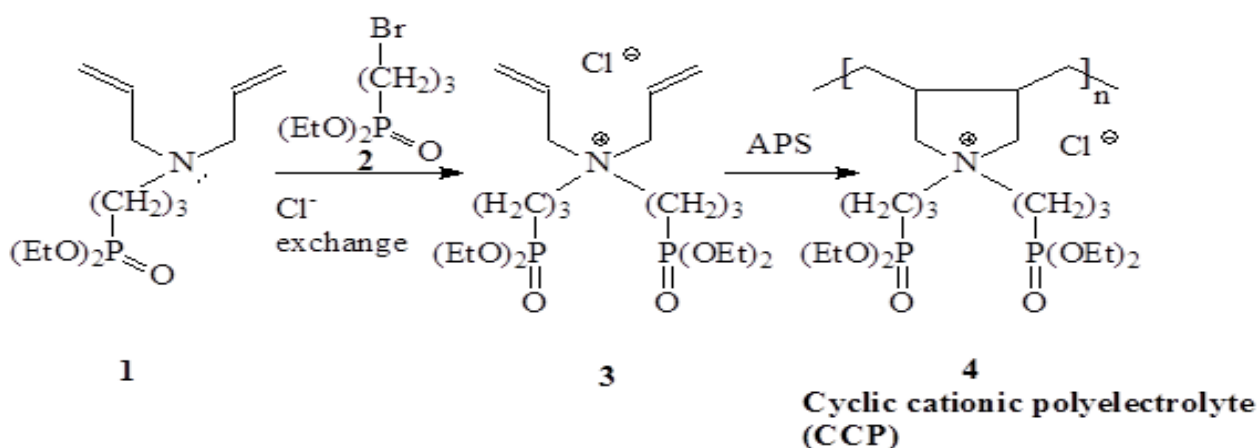
2. EXPERIMENTAL

2.1. Synthesis and characterization of CCP

2.1.1. Physical methods and materials

Elemental analyses were performed with the aid of Perkin Elmer Elemental Analyzer Series II Model 2400. The IR analysis was carried out using Perkin Elmer 16F PC FTIR spectrometer. The ^1H NMR, ^{13}C NMR, and ^{31}P NMR spectra were measured on a JEOL LA 500 MHz spectrometer in D_2O (using HOD signal at δ 4.65 and dioxane ^{13}C peak at δ 67.4 as internal standards). ^{31}P was referenced with 85% H_3PO_4 in dimethyl sulfoxide. Ammonium persulfate (APS) was purchased from Fluka AG (Buchs, Switzerland) and used as received. Monomer **3** was synthesized as reported [27]. HPLC grades solvents were used. A spectra/Por membrane (MWCO of 6000–8000 from Spectrum Laboratories) was used for dialysis.

The synthesis of CCP was carried out according to [27] with some modifications. A mixture of monomer **3** (5.4 g, 11 mmol), water (1.9 g) and APS (300 mg) was stirred for about 3 h at 95 °C in a 25 mL round-bottom flask. The reaction mixture was dialyzed against deionized water for 24 h and freeze-dried to yield CCP as light brown hygroscopic polymer (2.4 g, 44%). (Found: C, 48.7; H, 8.8; N, 2.8%. $\text{C}_{20}\text{H}_{42}\text{ClNO}_6\text{P}_2$ requires C, 49.03; H, 8.64; N, 2.86%); $\nu_{\text{max.}}(\text{KBr})$ 3420 (br), 2984, 2933, 2905, 1650, 1460, 1394, 1369, 1221, 1160, 1123, 1050, 1017, 968, 786, 698, 620 and 544 cm^{-1} . δ_{P} (202 MHz, D_2O): 32.89 (4%), 30.96 (72%), and 22.96 (24%). A synthetic pathway for obtaining CCP is displayed in scheme 1.



Scheme 1. Synthetic route for CCP

2.2. Corrosion inhibition studies

2.2.1. Materials and materials preparation

The metal substrate used in the study was low carbon steel with the following composition (wt%): C – 0.15; Mn – 1.26; V – 0.017; Si – 0.035; S – 0.008; Cr – 0.036; Ni – 0.03; Al – 0.083; Cu – 0.038; Fe – balance. The carbon steel was cut into coupons with dimensions of 3 cm × 3 cm × 0.25 cm. The specimens were abraded successively with different grits SiC paper starting with the coarsest (120) progressively to the finest (1000) grade, rinsed with distilled water, sonicated in ethanol bath at room temperature for 20 minutes for the removal polished residual particles, degreased with acetone and dried with warm air. Simulated corrosive environment was 15% HCl solution prepared by diluting AR grade 37% HCl (Sigma-Aldrich) with double distilled water. The synthesized polymer (CCP) was used as test corrosion inhibitor in the concentration range of 50 – 500 mg/L. The effect of ZnCl₂ (Sigma –Aldrich) and KI (Sigma –Aldrich) was assessed by introducing 5 mM of each additives into the inhibited solution containing 500 mg/L of CCP.

2.2.2. Weight loss measurements

Pre-cleaned low carbon steel samples were weighed using a digital analytical balance of ±0.1 mg sensitivity. They were loosely hanged in 250 ml test solutions in the absence and presence of different concentrations of CCP for 6 h. After this immersion time, the specimens were taken out and cleaned as previously reported [26] and reweighed. The difference in weight of the specimens before and after immersion in the various test solutions was taken as the weight loss. In order to assess the influence of temperature on the corrosion protection performance of CCP, the weight loss experiments were carried out at varying temperatures in the range between 25 and 60 °C.

The corrosion rate in terms of thickness loss (mm y⁻¹) and inhibition efficiency were computed from the weight loss data using equations (1) and (2) respectively:

$$C_R (\text{mm y}^{-1}) = \frac{87.6 \times \Delta W}{\rho A T} \quad (1)$$

$$\eta\% = \frac{C_{R(\text{blank})} - C_{R(\text{inh})}}{C_{R(\text{blank})}} \times 100 \quad (2)$$

where C_R is the corrosion rate, W is the average weight loss (mg), ρ is the density of mild steel specimen (g cm⁻³), A is the surface area of the specimen (cm²) and T is the exposure time (h); $C_{R(\text{blank})}$ and $C_{R(\text{inh})}$ are the corrosion rates in the absence and presence of the inhibitor respectively at the same temperature.

2.2.3. Electrochemical measurements

A Reference 600 Gamry potentiostat/galvanostat instrument with framework system consisting of ESA410 and DC105 software applications and Echem Analyst 6.0 for data fittings was used for these sets of experiments. The prepared steel specimen (exposed surface area = 0.7855 cm²) was

deployed as the working electrode. The counter electrode was a graphite rod while silver/silver chloride (Ag/AgCl) was used as the reference electrode. All measurements were done in stagnant oxygen-rich solutions at 25 °C. For EIS measurements, the working electrode was left in the test solution for an hour to achieve a cardinal requirement of steady state. The actual EIS experiments were carried out at E_{corr} (corrosion potential); the frequency range was 100 kHz – 100 mHz, while the signal amplitude perturbation was 10 mV. For PDP studies, the potential range in which experiments were performed was ± 250 mV versus E_{corr} and the scan rate was 0.5 mVs⁻¹. To get the corrosion current densities (i_{corr}), Tafel curves were projected to i_{corr} . For LPR studies, potential range in which the measurements were done was ± 15 mV relative to OCP (open circuit potential) and the current response was measured at a scan rate of 0.125 mV/s. To get LPR graphs, plots of over-potential and current data were made on a straight line scale. The slope of the graphs in the area of the E_{corr} gave R_p (polarization resistance).

2.2.4. Surface morphology

The metal specimens used for morphological assessment were prepared as previously described in Solomon and Umoren [24]. The cleaned steel surfaces exposed to 15% HCl in the absence and presence of 500 mg/L CCP alone and on addition of 5 mM ZnCl₂ and KI additives were scanned with JEOL JSM-6610 LV SEM operated at accelerating voltage of 20 kV. The component elements on these surfaces were determined with the aid of an electron dispersive spectroscopy (EDS) (Oxford EDS X-act Inca 350 system) coupled to SEM instrument.

3. RESULTS AND DISCUSSION

3.1. Synthesis and characterization of CCP

The cyclic cationic polyelectrolyte (CCP) was synthesized from the corresponding cationic monomer **3** via Butler's cyclopolymerization protocol. The polymer was obtained at reasonable yield which could be as a result of degradative chain transfer between the monomer and the polymer via the ethoxy groups attached to the P atom, which in turn afforded low molecular weight polymer whose significant amount escaped via the dialysis bag. Similar observations have been reported [34].

Fig. 1 shows the ¹H and ¹³C NMR spectra of monomer **3** and CCP. The presence of negligible amount of residual alkene on the spectra of CCP suggests the occurrence of some chain propagation without cyclization. The stereochemistry of the ring substituents at C_{b,b} in CCP as *cis* and *trans* (ratio: 75/25) obtained by the integration of the ¹³C as well as ³¹P peaks is similar to earlier findings [34].

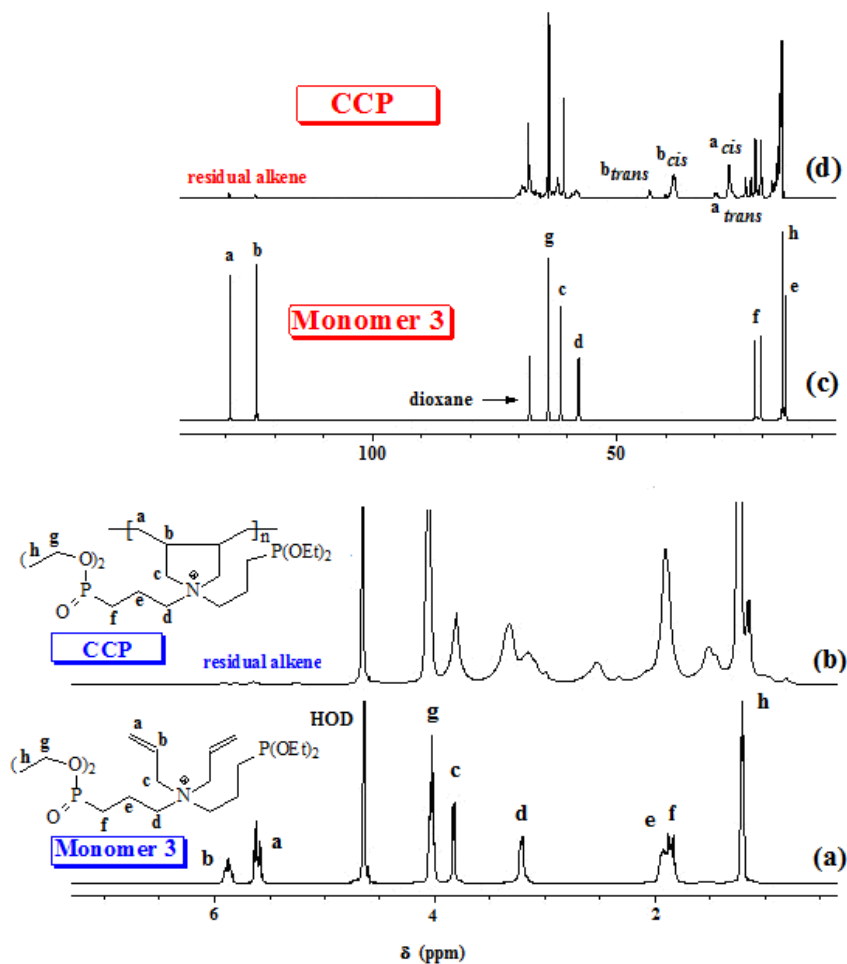


Figure 1. (a) ¹H NMR and (b) ¹³C NMR spectra of CCP

3.2. Corrosion inhibition effect of CCP

3.2.1. Weight loss measurements

Weight loss technique was utilized to assess the corrosion protection performance of CCP for carbon steel in 15% HCl. The effect of varying the concentration of CCP (50–500 mg L⁻¹) on the corrosion rate and inhibition efficiency for low carbon steel is illustrated in Fig. 2 (a) and (b), respectively. It is clear from Fig. 2(a) that the presence of CCP in the corrosive solution suppressed the dissolution of carbon steel significantly. Corrosion rate is observed to decrease while the inhibition efficiency increased with increasing CCP concentration. This suggests that, as the amount of CCP was raised, more of the CCP molecules were available for adsorption. This leads to greater portion of the metal surface being covered and protected from aggressive attack. The retardation in the corrosion rate and enhancement of the inhibition efficiency can be ascribed to the adsorption of the inhibitor molecules on the surface of the low carbon steel [35].

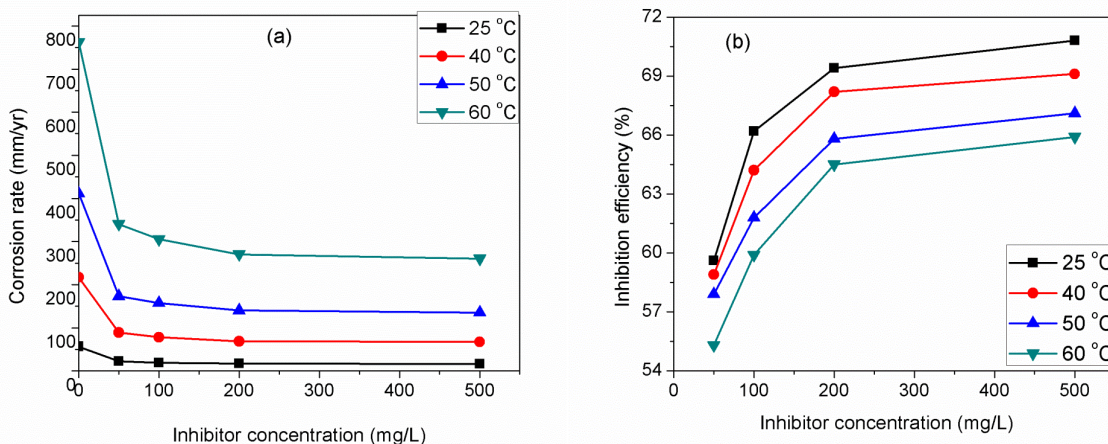


Figure 2. Variation of (a) corrosion rate and (b) inhibition efficiency with concentration of CCP for low carbon steel corrosion in 15% HCl at different temperatures from weight loss measurements

Examination of Fig. 2 also reveals that corrosion rate varies directly with temperature, that is, corrosion rate increase as the temperature increases whereas inhibition efficiency decreases with increase in temperature. The decrease in inhibition efficiency with increase in temperature can be attributed to the desorption of the molecules of CCP from the carbon steel surface.

3.2.2. Electrochemical measurements

The PDP curves for low carbon steel in 15% HCl free and containing varying concentrations of CCP are shown in Fig. 3. The associated parameters derived from the curves such as corrosion current density (i_{corr}), corrosion potential (E_{corr}), anodic Tafel slope (β_a), cathodic Tafel slope (β_c) and inhibition efficiency (η) are listed in Table 1. It follows from Fig. 3 that there is a decrease in the corrosion rate in the presence of the inhibitor, marked by a shift in the position of the anodic and cathodic current curves to lower current densities. The shifts in corrosion current are not remarkable with increase in concentration of CCP. The reduction in current density is seen to be approximately 10% from Table 1. The observed decrease in i_{corr} confirms the inhibitive nature of CCP. Based on the shift in the E_{corr} in the positive direction upon the addition of CCP, it suggests that CCP is anodic type inhibitor [36, 37]. However, considering the fact that the difference between the E_{corr} of the inhibited and uninhibited corrodent is less than 85 mV, which hitherto qualified it as anodic inhibitor, coupled with the shift in both anodic and cathodic current densities in the presence of CCP, it can be said that, CCP is a mixed-type inhibitor, affecting both anodic dissolution of metal and anodic evolution of hydrogen, having predominantly anodic effect [38, 39]. The protection efficiency from the PDP technique was calculated as follows:

$$\% \eta = \left(1 - \frac{i_{corr}}{i_{corr}^0} \right) \times 100 \tag{3}$$

where i_{corr}^0 and i_{corr} are the corrosion current densities without and with CCP respectively. The results are presented in Table 1 for the different concentrations of CCP investigated. From the table, there is an obvious increase in the protection efficiency with increase in CCP concentration reaching the value of 82.1% at the optimum concentration (500 ppm) studied.

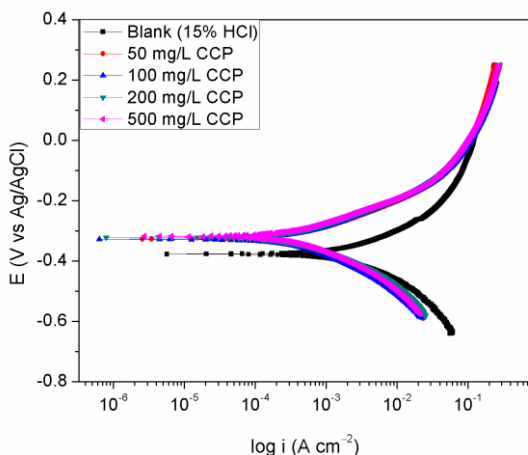


Figure 3. PDP curves for low carbon steel in 15% HCl in the absence and presence of different concentrations CCP at 25 °C

LPR method was also employed to study the corrosion protection performance of CCP for low carbon steel in 15% HCl solution. The inhibition efficiency (η) of CCP was determined using the following equation:

$$\eta\% = \left(1 - \frac{R_p^0}{R_p} \right) \times 100 \tag{4}$$

where R_p^0 and R_p are the polarization resistance values in the absence and presence of the inhibitor respectively. The values of the protection efficiency and polarization resistance with and without the addition of various concentrations of CCP are also given on Table 1.

Table 1. PDP and LPR parameters for low carbon steel in 15% HCl without and with CCP at 25 °C.

Concentration (mg/L)	E_{corr} (mV/SCE)	I_{corr} ($\mu A cm^{-2}$)	PDP method		IE (%)	LPR method	
			β_a (mV dec ⁻¹)	β_c (mV dec ⁻¹)		R_p (Ωcm^2)	IE (%)
Blank	-377	1975	107.9	118.4	-	14.4	-
50	-327	397	87.7	113.1	79.9	42.3	65.9
100	-327	377	89.7	114.4	80.9	50.9	71.7
200	-321	368	89.5	100.9	81.4	51.5	72.1
500	-317	354	88.8	110.1	82.1	54.1	73.3

As evident from the table, on the addition CCP, the polarization resistance increases relative to that of the uninhibited acid solution. This implies that CCP is a good inhibitor in the aggressive medium. The polarization resistance is also found to increase as the CCP concentration increases.

The obtained impedance results for corrosion measurement on low carbon steel in the absence and presence of different concentrations of CCP are presented in Fig. 4. In (a) Nyquist (b) Bode modulus and (c) Bode phase angle formats. Apparently from the figure, the Nyquist plots exhibit similar shape in the presence and absence of CCP suggesting that addition of the inhibitor does not change the corrosion mechanism. The Nyquist plots appear as depressed semicircles, a feature termed as frequency dispersion, which is ascribed to surface roughness and inhomogeneity of the solid surface [40, 41] as well as the geometrical behavior of the current distribution [42].

The impedance response of the system had been impacted by the addition of CCP. Clearly from the Nyquist plots (Fig. 4a), with respect to the control solution, there is an increase in the diameters of the semicircles as the concentration of CCP increases, which indicates corrosion inhibition behavior and adsorption of inhibitor molecules on the metal surface [42, 43]. Likewise, in the Bode plot (Fig. 4b), an increase in the absolute impedance at the low frequency region is observed with increase in concentration of CCP, confirming the greater protection as the concentration of CCP increases, which is related to the adsorption of inhibitors on the surface of the low carbon steel.

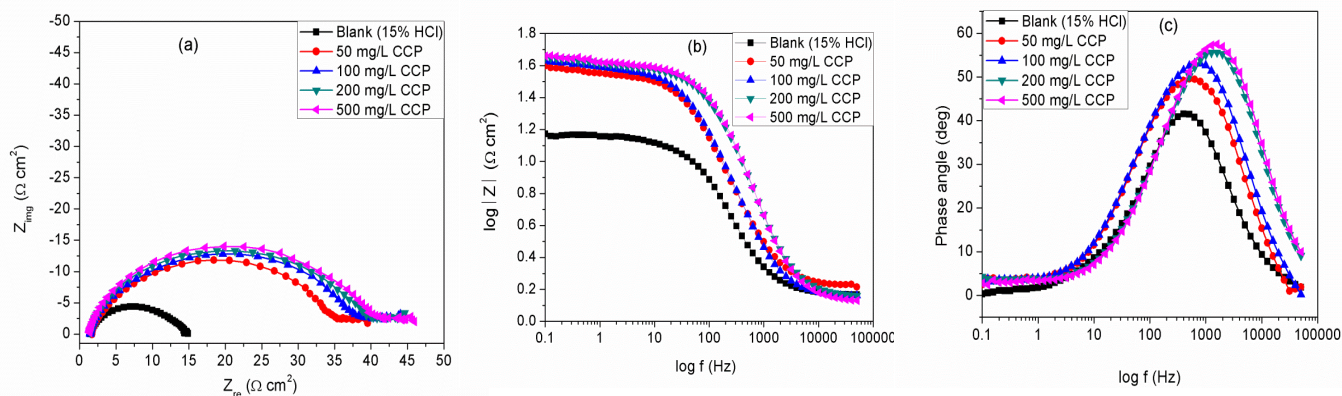


Figure 4. EIS plots for low carbon steel steel in 15% HCl in the absence and presence of different concentrations of CCP at 25 °C in (a) Nyquist, (b) Bode modulus and (c) Bode phase angle representations

To obtain the impedance parameters that characterize the electrochemical process, the impedance data were fitted into an equivalent circuit (Fig. 5) to model the impedance spectra. In the equivalent circuit (Fig. 5), CPE_f is the constant phase element related to the non-ideal capacitance of the inhibitor film and CPE_{dl} is the constant phase element that is related to the non-ideal capacitance of the double layer of the solution/corrosion products/metal interphase. R_f is the inhibitor film resistance, which reflects the protective properties of the inhibitor film. R_{ct} and R_s are the charge transfer and solution resistances respectively. The polarization resistance is evaluated using the equation:

$$R_p = R_{ct} + R_f \tag{5}$$

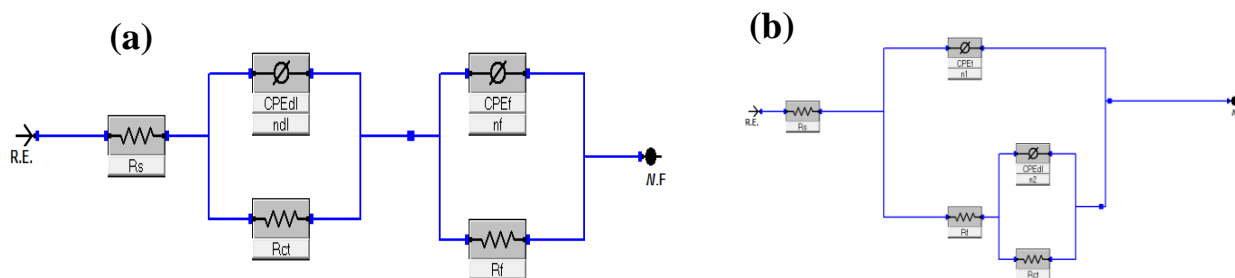


Figure 5. Equivalent circuit diagrams used to fit impedance data for (a) blank and others and (b) 5 mM ZnCl₂

In the simulation of the double layer capacitance (C_{dl}), a CPE is used since the double-layer largely behaves as a CPE instead of a pure capacitor [6]. The impedance of CPE is defined as:

$$Z_{CPE} = Y_o^{-1}(j\omega)^{-n} \tag{6}$$

where Y_o is a proportional factor that indicates the combination of properties related to both the surfaces and electroactive species independent of frequency; j is imaginary number ($\sqrt{-1}$); ω is the angular frequency and ω equal to $2\pi f$, where f is the frequency; and n has the meaning of a phase shift and is related to a slope of the $\log |Z|$ vs. $\log f$ plots and usually is in the range 0.5 and 1. The impedance parameters are given in Table 2. The inhibition efficacy and double layer capacitance were evaluated using Eqs. (7) and (8) respectively[44, 45]

$$\eta = \left(1 - \frac{R_p^0}{R_p} \right) \times 100 \tag{7}$$

$$C_{dl} = (2\pi f_{max} R_{ct})^{-1} \tag{8}$$

where R_p^0 and R_p are the polarization resistance values without and with CCP respectively and f_{max} is the frequency at which the imaginary component of the impedance is maximum.

Table 2. Impedance parameters for low carbon steel in 15% HCl without and with CCP at 25 °C.

Concentration (mg/L)	R_s (Ω cm ²)	CPE_f		R_f (Ω cm ²)	CPE_{dl}		R_{ct} (Ω cm ²)	R_p (Ω cm ²)	C_{dl} (μF cm ⁻²)	$\chi^2 \times 10^{-4}$	η (%)
		Y_o ($\mu\Omega s^n$ cm ⁻²)	n		Y_o (Ωs^n cm ⁻²) $\times 10^{-3}$	n					
Blank	1.45	340.2	0.85	9.85	8.94	0.76	3.36	13.21	187.7	7.5	–
50	1.59	131.5	0.81	32.44	67.69	0.62	8.23	40.67	154.0	14.3	67.5
100	1.35	110.8	0.82	34.67	41.56	0.62	9.87	44.53	128.4	13.8	70.3
200	1.32	87.1	0.84	35.15	33.83	0.59	10.09	45.24	62.5	81.4	70.8
500	1.24	74.45	0.85	35.87	25.38	0.62	9.53	45.39	52.9	6.2	70.9

From Table 2, it is seen that, the R_p and R_{ct} increase with increasing concentration of CCP. Additionally, the value of C_{dl} is found to decrease with respect to that of the blank. The higher R_{ct} and lower C_{dl} values is the consequence of increased diameter of the Nyquist semicircles. A high R_{ct} is

linked to a slower corroding system and a decreased C_{dl} is linked to a better protection rendered by an inhibitor [46]. Furthermore, the decrease in C_{dl} may be associated with the decrease of the local dielectric constant and/or increase in the thickness of the dielectric double layer suggesting that CCP reduces the metal corrosion by effective adsorption [47].

The decrease in C_{dl} values in the presence of CCP is in accordance with the Helmholtz model given by the equation:

$$C_{dl} = \frac{\epsilon\epsilon_0 A}{\delta} \quad (9)$$

where ϵ is the dielectric constant of the medium, ϵ_0 is the vacuum permittivity, A is the area of the electrode and δ is the thickness of the protecting layer. The inhibition efficiencies obtained by impedance studies (Table 2) are found to increase with increasing concentration of CCP and it happens to follow the same trend as those determined from PDP measurements.

3.2.3. Synergistic effect of $ZnCl_2$ and KI additives

Inhibitive synergism is defined as the reinforcement of inhibitive action of a compound, usually employed in higher concentrations, by the addition of a small amount of a second compound, even though the second compound is less effective when used alone [48]. The efficiency of many corrosion inhibitors has been reported to significantly improve when in combination with cations such as zinc ions and anions such as halides. For instance, the binary mixtures of zinc and different inhibitors like polymers, methionine, aminophosphonic acid, 2-mercaptobenzimidazol were found to exhibit synergistic effect [49-51]. Synergistic effect is, as well, known to exist between halides, especially iodides and various synthetic polymers [52-54].

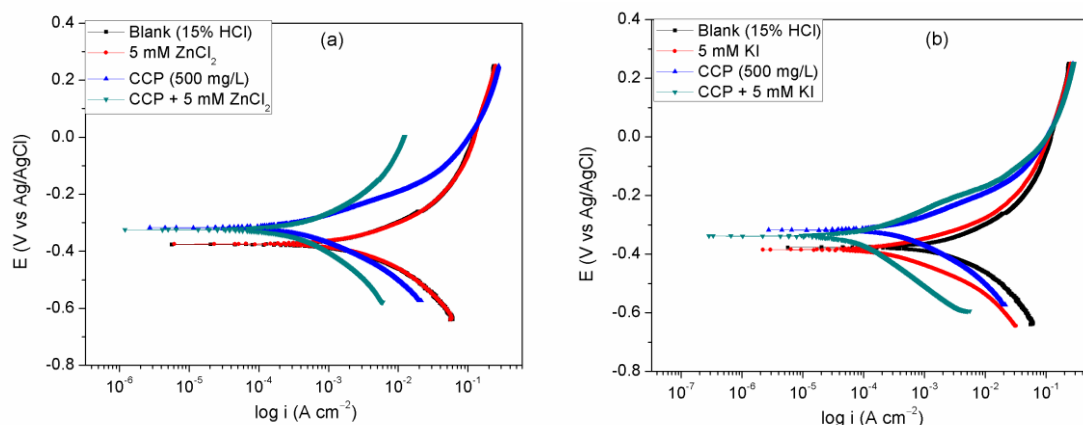


Figure 6. PDP curves for low carbon steel in 15% HCl in the absence and presence of (a) 5 mM $ZnCl_2$, CCP (500 mg/L) and CCP + 5 mM $ZnCl_2$ and (b) 5 mM KI, CCP (500 mg/L) and CCP + 5 mM KI at 25 °C.

Table 3. PDP and LPR parameters for low carbon steel in 15% HCl without, with 5 mM ZnCl₂, 5 mM KI, CCP and CCP in combination with 5 mM ZnCl₂ and 5 mM KI at 25 °C.

Concentration	PDP method					LPR method	
	E_{corr} (mV/SCE)	I_{corr} ($\mu\text{A cm}^{-2}$)	β_a (mV dec ⁻¹)	β_c (mV dec ⁻¹)	IE (%)	R_p (Ω cm ²)	IE (%)
Blank	-377	1975	107.9	118.4	–	14.4	–
5 mM ZnCl ₂	-375	1960	100.9	114.7	0.76	14.8	2.9
5 mM KI	-385	239	58.9	84.6	87.9	41.8	65.6
CCP (500 mg/L)	-317	354	88.8	110.1	82.1	54.1	73.3
CCP + 5 mM ZnCl ₂	-325	462	135.9	209.7	76.6	129.1	76.7
CCP + 5 mM KI	-338	70.2	69.2	146.6	96.4	293.3	95.1

PDP curves for low carbon steel in 15% HCl in the absence and presence of (a) 5 mM ZnCl₂, 500 mg/L of CCP and CCP in combination with 5 mM ZnCl₂ and (b) 5 mM KI, 500 mg/L of CCP and CCP - 5 mM KI mixtures are depicted Fig. 6a and b, respectively. The corresponding electrochemical parameters are listed in Table 3.

Inspection of the figures reveal a shift in corrosion potential in the positive direction on the addition of CCP in combination with ZnCl₂ (Fig. 6a) or KI (Fig. 6b) relative to the blank. From Table 3, it is seen that the addition of either of the binary inhibitor mixtures (CCP-ZnCl₂ or CCP-KI) to the strong acid is accompanied by a drastic decline in the corrosion current densities, in comparison to the blank solution and the solution with only CCP, the reduction is steeper for CCP-KI binary system. The above results imply that both binary mixtures, as well, behave as mixed inhibitors. Data in the table also show that the inhibition efficiency is improved for the binary formulations, CCP- ZnCl₂ (76.7%) and CCP-KI (95.1%), with respect to the additive-free CCP solution (73.3%) from LPR measurements. The enhancement in the corrosion inhibition efficiency of CCP on low carbon steel by both zinc and iodide ions are associated with synergistic effect. In the case where CCP-ZnCl₂ is added to the corrosive medium, the mechanism is attributed to the formation of CCP-Zn²⁺ complex which in turn forms a more protective and compact film on the steel surface[49, 55]. On the role played by the iodide ions in synergism, the iodide ions are said to get adsorbed on the metal surface thereby electrostatically attracting the positive end of the inhibitor molecule, thus, enhancing the corrosion protection capacity of the inhibitor [56, 57].

The impedance response plots of the low carbon steel/15% HCl system in the absence and presence of CCP and CCP in combination with 5 mM of ZnCl₂ are presented in Fig. 7. Similar plots are depicted in Fig. 8 for the low carbon steel/15% HCl solution in the presence and absence of CCP and CCP in combination with 5 mM of KI.

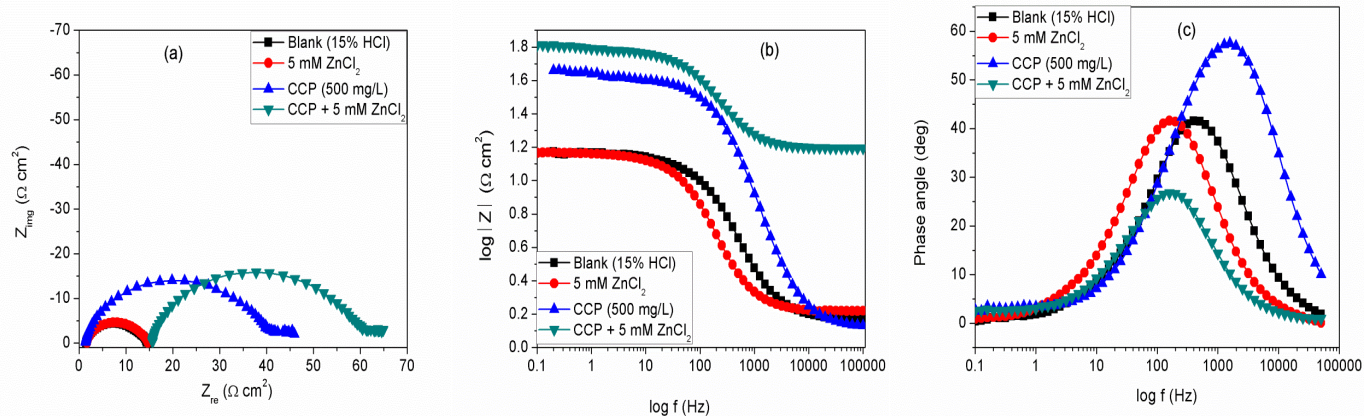


Figure 7. EIS plots for low carbon steel steel in 15% HCl in the absence and presence of 5 mM ZnCl₂, CCP (500 mg/L) and CCP + 5 mM ZnCl₂ at 25 °C in (a) Nyquist, (b) Bode modulus and (c) Bode phase angle representations.

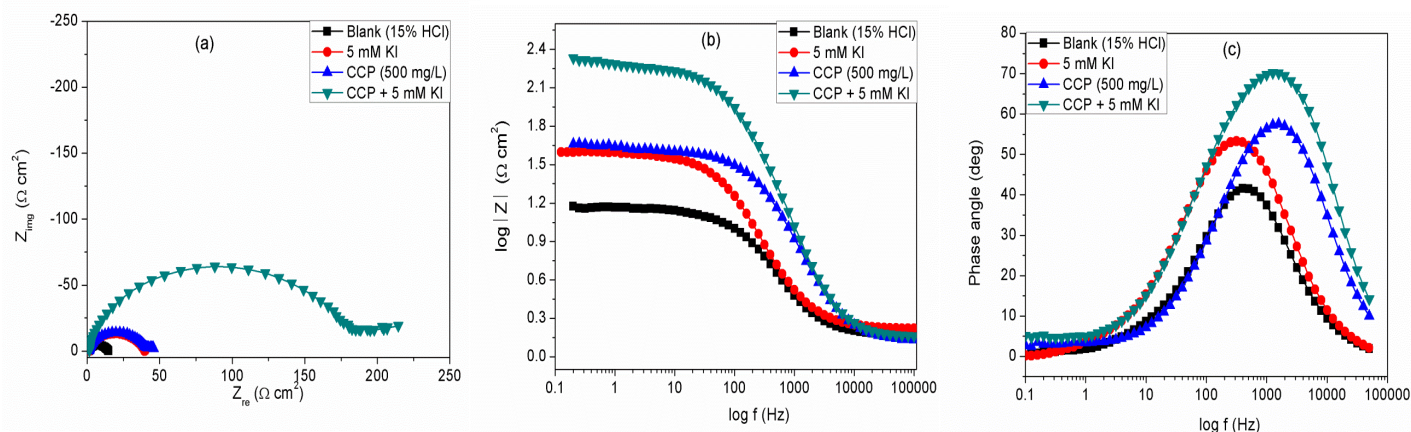


Figure 8. EIS plots for low carbon steel steel in 15% HCl in the absence and presence of 5 mM KI, CCP (500 mg/L) and CCP + 5 mM KI at 25 °C in (a) Nyquist, (b) Bode modulus and (c) Bode phase angle representations.

Table 4. Impedance parameters for low carbon steel in 15% HCl without, with 5 mM ZnCl₂, 5 mM KI, CCP and CCP in combination with 5 mM ZnCl₂ and 5 mM KI at 25 °C.

Systems/ concentrati on	R_s (Ω cm^2)	CPE _f			CPE _{dl}			R_p ($\Omega \text{ cm}^2$)	C_{dl} ($\mu\text{F cm}^{-2}$)	$\chi^2 \times 10^{-4}$	IE (%)
		Y_o ($\mu\Omega \text{ s}^n \text{ cm}^{-2}$)	n	R_f ($\Omega \text{ cm}^2$)	Y_o ($\Omega \text{ s}^n$ cm^{-2}) $\times 10^{-3}$	n	R_{ct} ($\Omega \text{ cm}^2$)				
Blank	1.45	340.2	0.85	9.85	8.94	0.76	3.36	13.21	187.7	7.5	–
5 mM ZnCl ₂	1.65	165.8	0.93	1.13	1.40	0.52	12.12	13.25	166.2	0.2	0.30
5 mM KI	1.62	161.7	0.85	29.53	3.71	0.79	8.60	38.13	123.4	83.4	65.4
CCP (500 mg/L)	1.24	74.45	0.85	35.87	25.38	0.62	9.53	45.39	52.9	6.2	70.9
CCP + 5 mM ZnCl ₂	15.36	98.9	0.81	42.52	55.34	0.50	11.36	53.88	111.6	0.95	75.5
CCP + 5 mM KI	1.32	27.5	0.93	91.26	2.3	0.59	103.0	194.26	15.4	17.9	93.2

Examination of the Nyquist plots (Fig. 7a and 8a) show that, upon introduction of the additives to CCP solution, the diameter of the semicircles increased significantly compared to that of CCP alone and the increase is much higher for the CCP+KI system. Similarly, a large increase in the impedance of the interface of the Bode plots was recorded (Fig. 7b and 8b). The corresponding values of the impedance parameters obtained using the same equivalent circuit shown in Fig. 5 are listed in Table 4. From the table, clearly the additives caused an increase in R_{ct} and a decrease in C_{dl} , which reflects the observed increased diameters of the semicircles in the Nyquist plots. The decline in C_{dl} results from increased double layer thickness which is linked to the synergistic effect between zinc ions, iodide ions and CCP.

Synergism parameter (S_1) determined using an equation reported elsewhere [58] was employed to assess the existence of synergistic inhibition effect between CCP+ZnCl₂ and CCP+KI. The calculated values of synergism parameter using different electrochemical techniques are presented in Table 5. The values of S_1 (Table 5) from potentiodynamic measurements are greater than unity for both additives. This confirms the existence of synergism between CCP and zinc ions as well as iodide ions.

Table 5. Synergism Parameter (S_1) for ZnCl₂ and KI at 25 °C from EIS, LPR and PDP measurements

Additives	Synergism parameter (S_1)		
	PDP method	LPR method	EIS method
ZnCl ₂	1.08	0.85	0.95
KI	1.77	1.47	1.47

3.2.4. Adsorption isotherm

Adsorption isotherms are often employed to describe the adsorption of a corrosion inhibitor, which in turn enables the understanding of the nature of the metal-inhibitor interaction. The commonly used isotherms models include: Langmuir, Temkin, Frumkin, Flory–Huggins, Bockris–Swinkels, Dhar–Flory–Huggin to mention but a few. The values of degree of surface coverage (θ) obtained from weigh loss technique for different concentrations of CCP were theoretically fitted to some of the adsorption isotherm models; in order to describe the adsorption of CCP on low carbon steel in 15% HCl. The degree of surface coverage was calculated using $\theta = \eta/100$ and the results obtained fit well to Langmuir adsorption isotherm model characterized by:

$$\frac{C}{\theta} = \frac{1}{K_{ads}} + C \quad (10)$$

where C is the concentration, θ is the degree of surface coverage, K_{ads} is the equilibrium constant of the adsorption-desorption process and can be calculated from the intercepts of the plot of C/θ vs C (Fig. 9) and K_{ads} is related to standard free energy of adsorption, ΔG_{ads}^0 , according to:

$$\Delta G_{ads}^0 = -RT \ln(1 \times 10^6 K_{ads}) \quad (11)$$

where R is the universal gas constant, T is the absolute temperature and 1×10^6 is the concentration of water molecules expressed in mg L⁻¹ or ppm

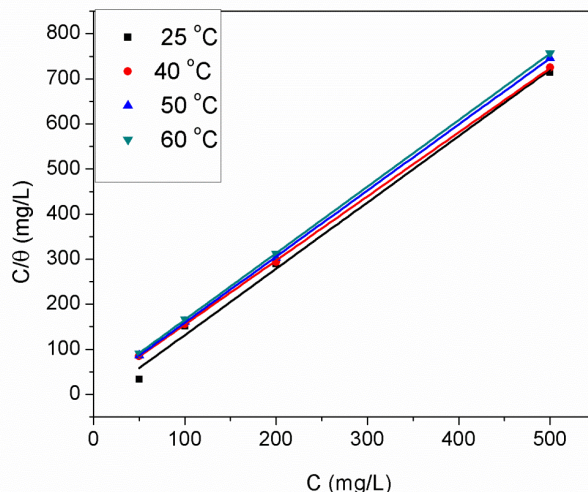


Figure 9. Langmuir adsorption isotherm for low carbon steel in 15% HCl containing CCP at different temperatures from weight loss measurements.

Fig. 9 displays the plot of the Langmuir isotherm model. The obtained linear plot has a very good regression coefficient (0.999) indicating that the adsorption of CCP on low carbon steel is well described by Langmuir isotherm. The isotherm assumes that no interaction between the adsorbed species occur on the electrode surface [59]. The adsorption parameters obtained from Langmuir plot are collected in Table 6.

Table 6. Langmuir adsorption parameters for low carbon steel in 15% HCl containing CCP at different temperatures from weight loss measurements.

Temperature (°C)	$\Delta G_{\text{ads}}^{\circ}$ (kJ mol ⁻¹)	K_{ads} (L mg ⁻¹) × 10 ⁻²	slope	R ²
25	-27.46	6.25	1.47	0.993
40	-29.31	7.84	1.42	0.999
50	-30.87	7.84	1.47	0.999
60	-30.29	5.66	1.48	0.999

It is noted from the table that slope obtained from the Langmuir isotherm plot is more than unity suggesting interactions between the adsorbed inhibitor molecules and negating the Langmuir postulates of monolayer inhibitor film formation on the steel surface. This is not surprising given the fact that CCP are macromolecules with multiple adsorption centres/sites that may adsorbed differently on the metal surface. Such adsorbed species may interact by mutual repulsion or attraction. Similar observations have been reported in our earlier studies employing long chain polymer molecules for carbon steel in acidic medium [22, 60]. The negative ΔG value is associated with spontaneous adsorption process and stable adsorbed film on the surface of the low carbon steel [61]. It is widely believed that a value of $\Delta G_{\text{ads}}^{\circ}$ around -20 kJ/mol or lower signifies a physisorption process, which is an electrostatic interaction between the inhibitor and the charged metal surface, and a value of around -40 kJ mol⁻¹ or higher indicates a chemisorption process characterized by charge sharing or transfer

between the inhibitor molecule and the metal surface [62]. The values of ΔG calculated for the adsorption of CCP on low carbon steel fall in the range $-27.46 \text{ kJ mol}^{-1}$ to $-30.87 \text{ kJ mol}^{-1}$ in the temperature range (25-60 °C). Therefore, based on these data, the adsorption could be accompanied by both physisorption and chemisorption processes.

3.2.5. Effect of temperature

The variation of corrosion rate and inhibition efficiency with concentration at different temperatures for CCP from weight loss measurements is presented on Fig. 2. Clearly the inhibition efficiency decreases with the rise of temperature, while the corrosion rate increases as the temperature increases.

The dependence of corrosion rate on temperature can be expressed by Arrhenius equation:

$$\text{Log } C_R = \log A - \left(\frac{E_a}{2.303RT} \right) \quad (12)$$

where C_R is the corrosion rate, E_a is the apparent activation energy, R is the molar gas constant, T is the absolute temperature, and A is the frequency factor. The plot of $\log C_R$ against $1/T$ is depicted in Fig. 10 and appeared to be linear with correlation coefficient (R^2) close to unity indicating that Arrhenius equation is obeyed. The values of E_a obtained from the slope of Arrhenius plot (Fig. 10) are listed in Table 7.

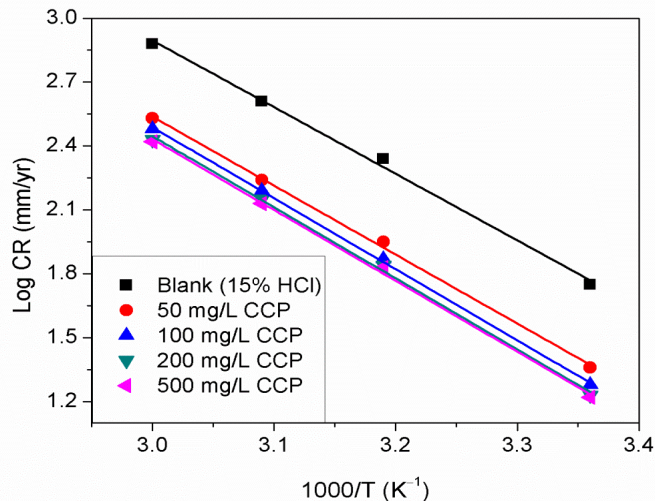


Figure 10. Arrhenius plot of $\text{Log } C_R$ versus $1/T$ for low carbon steel in 15% HCl in the absence and presence of different concentrations of CCP.

Examination of the table showed that for all the concentrations of CCP, the activation energy increased with respect to the blank. In such a case where the E_a of an inhibitor increased compared to the blank, physical adsorption may be considered [63]. A decrease or no change in energy is attributed to chemisorption. It is believed that the existence of mixed adsorption should be accompanied by little or no changes in the activation energy, and generally, upward or downward changes might be linked to

advantageous physical or chemical bonding[64]. The activation energy variation obtained for CCP is in conformity with those reported earlier[64]. It has been opined that the increase in the E_a resulted from an appreciably diminished adsorption of the inhibitor molecule on the surface of the steel as the temperature rises [65]. In order to preserve the adsorption/desorption equilibrium; as the adsorption of the inhibitor molecules decreases, the desorption will ultimately increase. Hence, the occurrence of more desorption of the inhibitor molecules at higher temperatures will expose a greater surface area of the steel to the corrosive medium, leading to increased corrosion rate with increase in temperature [66, 67].

The activation enthalpy and entropy of corrosion for the low carbon steel-HCl system in the presence and absence of CCP were obtained from the equation of Transition State Theory given by:

$$\log\left(\frac{C_R}{T}\right) = \left[\log\left(\frac{R}{Nh}\right) + \left(\frac{\Delta S^*}{2.303R}\right) \right] - \frac{\Delta H^*}{2.303RT} \tag{13}$$

where $N(6.02252 \times 10^{23} \text{ mol}^{-1})$ is the Avogadro's number, $h(6.626176 \times 10^{-34} \text{ Js})$ is the Planck's constant, R and T retain the earlier meanings.

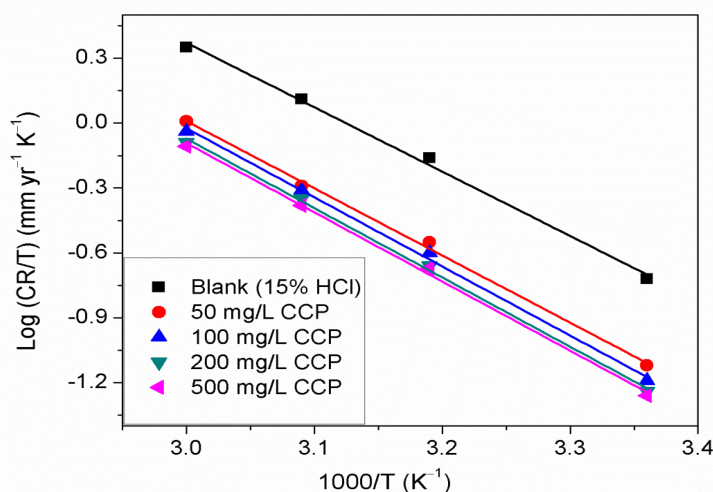


Figure 11. Transition state plot of $\text{Log } C_R$ versus $1/T$ for low carbon steel in 15% HCl in the absence and presence of different concentrations of CCP.

Table 7. Activation parameters for low carbon steel corrosion in 15% HCl in the absence and presence of different concentrations of CCP.

Concentration (mg/L)	E_a (kJ mol ⁻¹)	ΔH^* (kJ mol ⁻¹)	$-\Delta S^*$ (J mol ⁻¹ K ⁻¹)
Blank	59.88	56.98	19.52
50	62.85	59.46	19.01
100	63.82	61.19	14.42
200	63.85	61.38	14.81
500	63.66	61.24	15.62

The Transition State plots for low carbon steel corrosion in 15% HCl solution without and with CCP are illustrated on Fig. 11 as $\log(C_R/T)$ vs $1/T$. Straight line graphs with correlation coefficient close to unity were obtained with slope of $-\Delta H^*/2.303R$ and intercept of $\log(R/Nh) + (\Delta S^*/2.303R)$ from which the values of enthalpy of activation (ΔH^*) and entropy of activation (ΔS^*), respectively, were calculated and presented also in Table 7.

It is observed that the magnitudes of ΔH^* and E_a are close and vary in similar fashion. They increased with increase in concentration of CCP reaching a maximum and after that remain virtually constant. Based on this behavior, the decrease in corrosion rate of the low carbon steel by CCP is considered to be mainly controlled by activation parameters [64]. The activation entropy becomes less negative in the presence of CCP indicating that there is an increase in randomness during the transition from reactants to activated complex [68].

3.2.6. Surface morphology

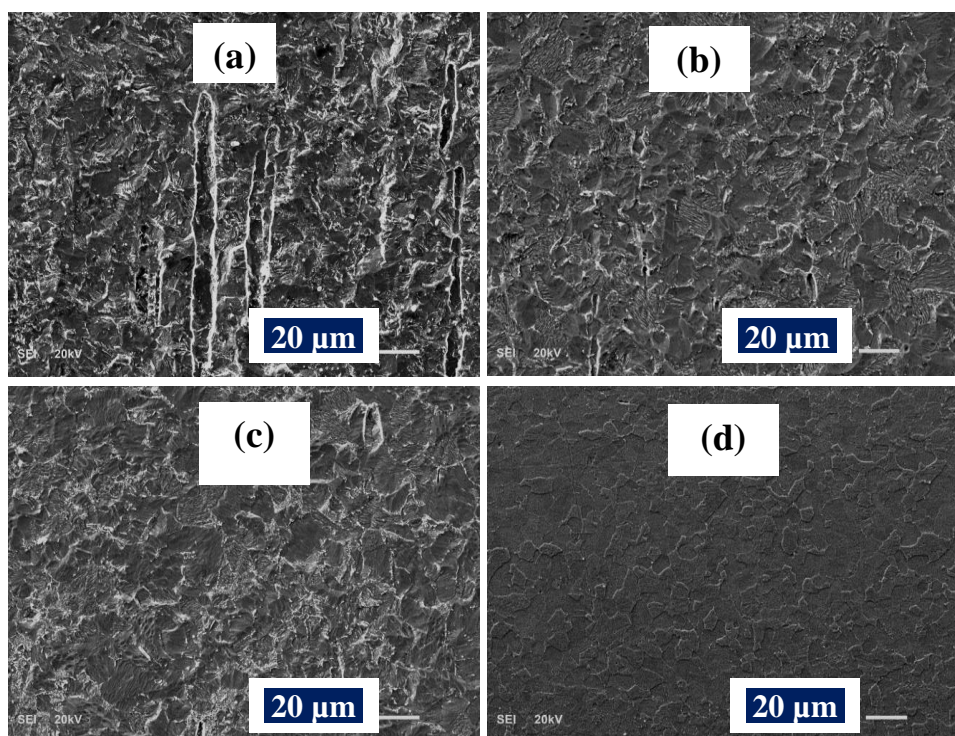


Figure 12. SEM micrographs for carbon low steel exposed to (a) 15% HCl, (c) 15% HCl containing 500 mg/L CCP, (c) 15% HCl containing 500 mg/L CCP + 5mM ZnCl₂ and (d) 15% HCl containing 500 mg/L CCP + 5mM KI after 12 h immersion.

The SEM images of low carbon steel after 12 h immersion in 15% HCl and 15% HCl containing 500 mg/L CCP are shown in Fig. 12a and b respectively. It is seen that the degree of surface morphological damage on the blank sample is higher compared to that in CCP solution. This indicates that in the presence of CCP a protective film was formed on the low carbon steel. The surface damage of the low carbon steel further reduces when immersed in the strong acid solution containing CCP in combination with 5mM ZnCl₂ (Fig. 12c). Furthermore, observation of Fig. 12d reveals that the surface

of the low carbon steel is relatively best protected by CCP in combination with 5mM KI. The enhanced surface protection justified the contribution of the additives toward better adsorption of CCP on the surface of the steel.

EDS analysis of the surface of the low carbon steel was also carried out before and after immersion in 15% HCl and CCP solution alone and CCP in combination with the additives. The EDS results obtained are presented in Fig. 13a-d. It could be seen from the figures that the percentage atomic content of Fe is lowest (86.1%) in the sample immersed in the inhibitor-free solution in comparison to the percentage of those immersed in the inhibited solutions. This is due to the dissolution of Fe caused by corrosion attack by the aggressive medium. The highest percentage of Fe (92.6%) is recorded from the EDS spectrum of the steel inhibited with CCP in combination with KI. The percentages of Fe obtained in the presence of CCP and CCP with $ZnCl_2$ are 89% and 91.5% respectively. This implied that CCP film was formed on the steel surface and the film formation was augmented by zinc and iodide ions.

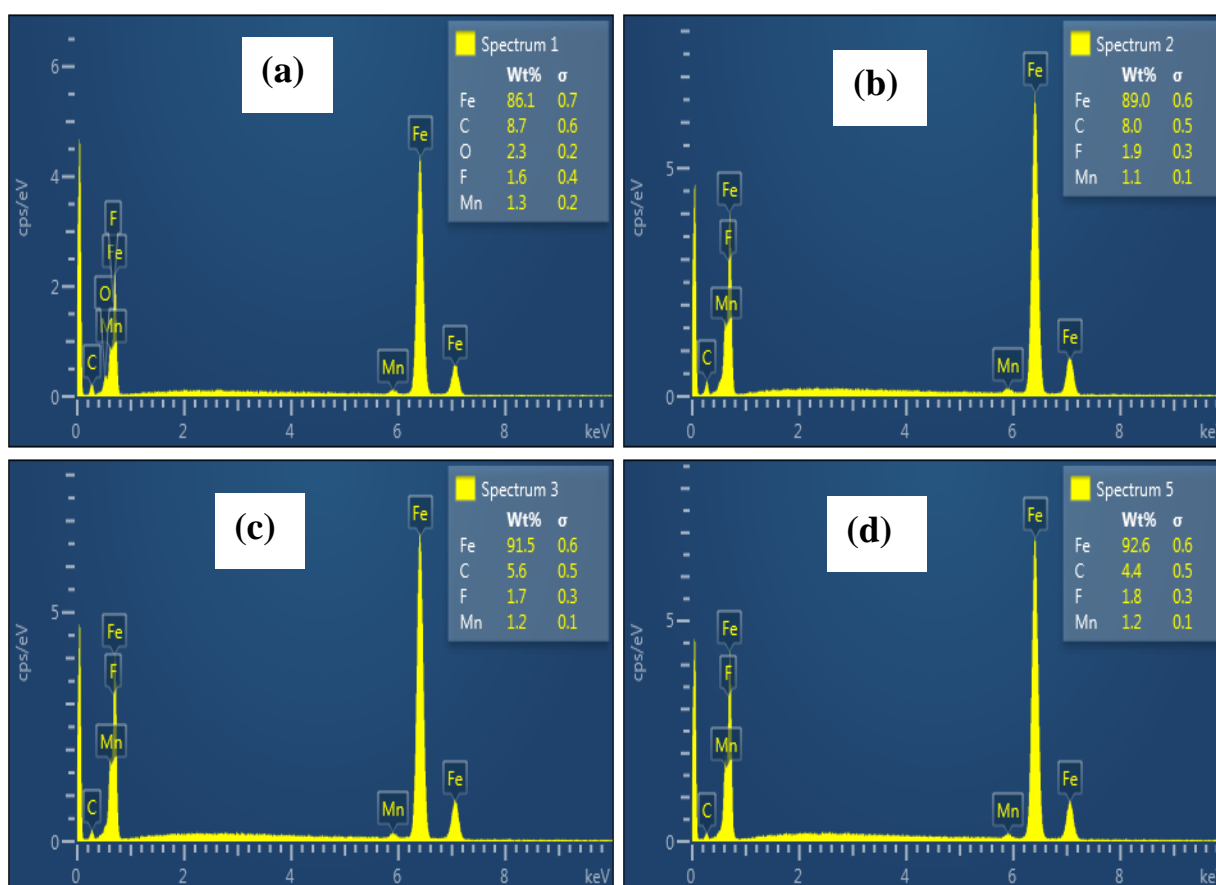


Figure 13. EDS micrographs for low carbon steel exposed to (a) 15% HCl, (c) 15% HCl containing 500 mg/L CCP, (c) 15% HCl containing 500 mg/L CCP + 5mM $ZnCl_2$ and (d) 15% HCl containing 500 mg/L CCP + 5mM KI after 12 h

3.2.7. Mechanism of corrosion inhibition

The corrosion inhibition performance of CCP on low carbon steel in 15% HCl can be explained on the basis of molecular interaction between CCP and the metal surface. CCP already bears a

permanent positively charged nitrogen atom on each repeating unit. The positive site aids in the adsorption of CCP on the cathodic sites of the low carbon steel, thereby inhibiting the evolution of hydrogen [28]. Additionally, the negatively charged metal surface rendered by the adsorption of Cl^- ions from the acid will interact with the positive end of the polymer and inhibit corrosion. Adsorption on the anodic site of the steel occurs via the unshared electron pairs on the phosphorus and oxygen atom to form a bond with the vacant d-orbitals of iron on the metal surface.

With respect to KI additive to CCP, it is a common occurrence which has been widely reported in the corrosion inhibition literature that the presence of halide ions in acidic media synergistically increases the inhibition efficiency of some organic compounds[69]. In the present study, the iodide ions are able to improve adsorption of the CCP cations by forming intermediate bridges between the positively charged metal surface and the positive end of the organic inhibitor. Corrosion inhibition synergism thus results from the increased surface coverage arising from the ion-pair interactions between the organic cations and anions. According to Fishtik and co-workers [70], there are two ways in which the ion-pairs can be adsorbed on the metal surface. In one way, the ion pairs are formed in the bulk of the solution and then adsorbed from the solution onto the metal surface. In the second way, the iodide ion is first adsorbed on the metal surface and the inhibitor is then drawn into the double layer by the adsorbed iodide ion such that the ion pair formation occurs directly on the metal surface. In the case of ZnCl_2 additive, it is generally believed that the formation of Zn^{2+} – inhibitor complex which ensures wider surface coverage is responsible for the usual observed synergistic inhibition effect. The synergistic corrosion inhibition effect of Zn^{2+} and inhibitor formulation is found to be influenced by the concentration of Zn^{2+} ions in solution, pH of the corrosive medium and immersion time. The poor synergistic inhibition effect of Zn^{2+} addition to CCP could be attributed to the solution low pH. In the highly acidic medium, the inhibitor molecules may be protonated and the protonated species may not coordinate with Zn^{2+} as effectively as the deprotonated molecules due to the repulsive force that will be exerted by the charged species, as a consequence the protective complex may not form.

4. CONCLUSIONS

The following conclusions can be drawn from the findings of this work:

1. The synthesized cyclic cationic polymer (CCP) has been found to be effective corrosion inhibitor for low carbon steel in 15% HCl.
2. The inhibition efficiency increases with increase in concentration of CCP and declines with increase in temperature.
3. Combination of CCP with zinc and iodide ions significantly improved the inhibition efficiency through synergistic effect, with iodide ions showing stronger synergistic effect.
4. The potentiodynamic polarization measurements suggest that CCP act as a mixed inhibitor but with a predominant influence on anodic reaction.
5. The results of impedance measurement show that the double layer capacitance (C_{dl}) decreases and the charge transfer resistance (R_{ct}) increases on the addition of CCP, indicating the adsorption of CCP on the steel surface.

6. The adsorption of CCP on the low carbon steel was found to obey Langmuir adsorption isotherm model.
7. The trend of η with temperature and the values of kinetic/thermodynamic parameters obtained from the experimental data favor the phenomenon of both physisorption and chemisorption.
8. SEM-EDS analysis results confirm the formation of CCP film on the surface of the steel.

ACKNOWLEDGEMENTS

The authors gratefully acknowledged the financial support provided by University of Dammam (UoD) through project number: 2016-237-Eng. Some research facilities provided by Centre of Research Excellence in Corrosion, KFUPM are thankfully acknowledged.

References

1. M. A. Migahed, I. F. Nassar, *Electrochim. Acta*, 53 (2008) 2877.
2. M. Yadav, R. R. Sinha, S. Kumar, T. K. Sarkar, , *RSC Adv.*, 5 (2015) 70832.
3. N. Haldar, H.S. Shukla, G. Udayabhanu, *Ind. J. Chem. Techn.*, 19 (2012) 173.
4. D. Jayaperumal, *Mater. Chem. Phys.*, 119 (2010) 478.
5. M. Yadav, D. Behera, S. Kumar, R. R. Sinha, *Ind. Eng. Chem. Res.*, 52 (2013) 6318.
6. M. A. Amin, K. F. Khaled, Q. Mohsen, H. A. Arida, *Corros. Sci.*, 52 (2010) 1684.
7. M. Heydari, M. Javidi, , *Corros. Sci.*, 61 (2012) 148.
8. M. Yadav, L. Gope, N. Kumari, P. Yadav, *J. Mol. Liq.*, 216 (2016) 78.
9. G. Cabello, G.P. Funkhouser, J. Cassidy, C.E. Kiser, J. Lane, A. Cuesta, *Electrochim. Acta*, 97 (2013) 1.
10. M. Yadav, S. Kumar, R. R. Sinha, S. Kumar, *J. Dispers. Sci. Techn.*, 35 (2014) 1751.
11. H. M. Abd El-Lateef, M. A. Abo-Riya, A. H. Tantawy, *Corros. Sci.*, 108 (2016) 94.
12. K. R. Ansari, M. A. Quraishi, A. Singh, *Measurement*, 76 (2015) 136.
13. K. R. Ansari, M. A. Quraishi, A. Singh, S. Ramkumar, I. B. Obot, *RSC Adv.*, 6 (2016) 24130.
14. M. Behpour, S.M. Ghoreishi, M. Salavati-Niasari, B. Ebrahimi, *Mater. Chem. Phys.*, 107 (2008) 153.
15. Z. Yang, F. Zhan, Y. Pan, Z. Lyu, C. Han, Y. Hu, P. Ding, T. Gao, X. Zhou, Y. Jiang, *Corros. Sci.*, 99 (2015) 281.
16. M. Yadav, S. Kumar, L. Gope, *J. Adhes. Sci. Technol.*, 28 (2014) 1072.
17. M. Bello, N. Ochoa, V. Balsamo, F. López-Carrasquero, S. Coll, A. Monsalve, G. González, *Carbohydr. Polym.*, 82 (2010) 561.
18. L. A. A. Juhaiman, A. A. Mustafa, W. K. Mekhamer, *Anti-Corros. Methd Mater.*, 60 (2013) 28.
19. M. M. Solomon, S. A. Umoren, I. I. Udosoro, A. P. Udoh, *Corros. Sci.*, 52 (2010) 1317.
20. D. Thirumoolan, V. A. Katkar, G. Gunasekaran, T. Kanai, K. Anver Basha, *Prog. Org Coat.*, 77 (2014) 1253.
21. R. Baskar, D. Kesavan, M. Gopiraman, K. Subramanian, *Prog. Org. Coat.*, 77 (2014) 836.
22. S. A. Umoren, I. B. Obot, A. Madhankumar, Z. M. Gasem, *Carbohydr. Polym.*, 124 (2015) 280.
23. M. Vakili Azghandi, A. Davoodi, G. A. Farzi, A. Kosari, *Corros. Sci.*, 64 (2012) 44.
24. M. M. Solomon, S. A. Umoren, *J. Adhes. Sci. Techn.*, 29 (2015) 1060..
25. A. Biswas, S. Pal, G. Udayabhanu, *Appl. Surf. Sci.*, 353 (2015) 173.
26. S. A. Umoren, *J. Mol. Liq.*, 219 (2016) 946.
27. S. A. Ali, S. A. Haladu, H. A. Al-Muallem, *J. Appl. Polym. Sci.*, 131 (2014) 40615.

28. M. Yadav, D. Sharma, S. Kumar, I. Bahadur, E. E. Ebenso, *Int. J. Electrochem. Sci.*, 9 (2014) 6580.
29. K. Kavipriya, S. Rajendran, A. S. Prabha, *Eur. Chem. Bull.*, 1 (2012) 366.
30. G. Gunasekaran, R. Natarajan, V. S. Muralidharan, N. Palaniswamy, B. V. A. Rao, *Anti-Corros. Methd. Mater.*, 44 (1997) 248.
31. C. E. De, , *Annu. Rev. Pharmacol. Toxicol.*, 51 (2011) 1.
32. H. Fleish, W. F. Neuman, *Am. J. Physio.*, 200 (1961) 1296.
33. N. Moszner, T. Hirt, *J. Polym. Sci. Part A: Polym. Chem.*, 50 (2012) 4369.
34. S. A. Ali, N. Y. Abu-Thabit, H. A. Al-Muallem, *J. Polym. Sci., Part A: Polym. Chem.*, 48 (2010) 5693.
35. C. Verma, L. O. Olasunkanmi, I. B. Obot, E. E. Ebenso, M. A. Quraishi, *RSC Adv.*, 6 (2016) 15639.
36. M. A. J. Mazumder, H. A. Al-Muallem, M. Faiz, S. A. Ali, *Corros. Sci.*, 87 (2014) 187.
37. R. Cui, N. Gu, C. Li, *Mater. Corros.*, 62 (2011) 362.
38. N. K. Gupta, C. Verma, M. A. Quraishi, A. K. Mukherjee, *J. Mol. Liq.*, 215 (2016) 47.
39. D. Yang, M. Zhang, J. Zheng, H. Castaneda, , *RSC Adv.*, 5 (2015) 95160-95170.
40. J. R. Macdonald, , *J. Electroanal. Chem. Interf. Electrochem.*, 223 (1987) 25.
41. A. Dutta, S.K. Saha, P. Banerjee, A.K. Patra, D. Sukul, *RSC Adv.*, 6 (2016) 74833-74844.
42. B. Zhang, C. He, C. Wang, P. Sun, F. Li, Y. Lin, *Corros. Sci.*, 94 (2015) 6.
43. D. K. Yadav, D. S. Chauhan, I. Ahamad, M. A. Quraishi, *RSC Adv.*, 3 (2013) 632.
44. M. V. Fiori-Bimbi, P. E. Alvarez, H. Vaca, C. A. Gervasi, *Corros. Sci.*, 92 (2015) 192.
45. S. A. Umoren, Y. Li, F. H. Wang, , *Corros. Sci.*, 52 (2010) 2422.
46. D. A. López, S. N. Simison, S. R. de Sánchez, *Electrochim. Acta*, 48 (2003) 845.
47. B. Xu, Y. Ji, X. Zhang, X. Jin, W. Yang, Y. Chen, *RSC Adv.*, 5 (2015) 56049.
48. G. Gunasekaran, R. Natarajan, N. Palaniswamy, *Corros. Sci.*, 43 (2001) 1615.
49. D. Q. Zhang, Q. R. Cai, X. M. He, L. X. Gao, G. S. Kim, *Mater. Chem. Phys.*, 114 (2009) 612.
50. J. Telegdi, M. M. Shaglouf, A. Shaban, F. H. Kármán, I. Betróti, M. Mohai, E. Kálmán, *Electrochim. Acta*, 46 (2001) 3791.
51. M. H. Wahdan, *Mater. Chem. Phys.*, 49 (1997) 135.
52. L. Larabi, Y. Harek, M. Traisnel, A. Mansri, *J. Appl. Electrochem.*, 34 (2004) 833.
53. S. A. Umoren, E. E. Ebenso, *Mater. Chem. Phys.*, 106 (2007) 387.
54. C. Jeyaprabha, S. Sathiyarayanan, S. Muralidharan, G. Venkatachari, , *J. Braz. Chem. Soc.*, 17 (2006) 61.
55. M. Prabakaran, K. Vadivu, S. Ramesh, V. Periasamy, *Egypt. J. Petrol.*, 23 (2014) 367.
56. S. A. Umoren, M. M. Solomon, I. I. Udosoro, A. P. Udoh, *Cellulose*, 17 (2010) 635.
57. S. A. Umoren, I. B. Obot, *J. Adhes. Sci. Techn.*, 28 (2014) 2054.
58. S. A. Umoren, M. M. Solomon, U. M. Eduok, I. B. Obot, A. U. Israel, *J. Environ. Chem. Eng.*, 2 (2014) 1048.
59. M. Elayyachy, A. El Idrissi, B. Hammouti, *Corros. Sci.*, 48 (2006) 2470-2479.
60. S. A. Umoren, Z. M. Gasem, *J. Dispers. Sci. Techn.*, 35 (2014) 1181.
61. H. Keleş, M. Keleş, İ. Dehri, O. Serindağ, *Coll. Surf. A: Physicochem. Eng. Aspects*, 320 (2008) 138.
62. F. Bentiss, C. Jama, B. Mernari, H. E. Attari, L. E. Kadi, M. Lebrini, M. Traisnel, M. Lagrenée, *Corros. Sci.*, 51 (2009) 1628.
63. S. Martinez, I. Stern, *Appl. Surf. Sci.*, 199 (2002) 83.
64. A. K. Singh, M. A. Quraishi, *Corros. Sci.*, 52 (2010) 1373-1385.
65. T. Szauer, A. Brandt, *Electrochim. Acta*, 26 (1981) 1253-1256.
66. T. Szauer, A. Brandt, *Corros. Sci.*, 23 (1983) 1247.
67. H. Zarrok, A. Zarrouk, B. Hammouti, R. Salghi, C. Jama, F. Bentiss, *Corros. Sci.*, 64 (2012) 243.
68. A. Yurt, A. Balaban, S.U. Kandemir, G. Bereket, B. Erk, *Mater. Chem. Phys.*, 85 (2004) 420.

69. E. E. Oguzie, Y. Li, F. H. Wang, *J. Coll. Interf. Sci.*, 310 (2007) 90.

70. I. F. Fishtik, I. I. Vataman, F. A. Spatar, *J. Electroanal. Chem. Interf. Electrochem.*, 165 (1984) 1.

© 2017 The Authors. Published by ESG (www.electrochemsci.org). This article is an open access article distributed under the terms and conditions of the Creative Commons Attribution license (<http://creativecommons.org/licenses/by/4.0/>).